

# Voltage Oscillations in a Polymer Electrolyte Membrane Fuel Cell with Pd-Pt/C and Pd/C Anodes

Jéssica Alves Nogueira and Hamilton Varela\*<sup>[a]</sup>

Polymer electrolyte membrane fuel cells (PEMFC) fed with H<sub>2</sub> contaminated with CO may exhibit oscillatory behavior when operated galvanostatically. The self-organization of the anodic overpotential is interesting because it can be accompanied by an increase in the average performance. Herein we report experimental studies of voltage oscillations that emerge in a PEMFC equipped with a Pd/C or PdPt/C anode and fed with H<sub>2</sub> contaminated with CO (100 ppm). We used on-line mass spectrometry to investigate how the mass fragments associated with CO<sub>2</sub> and CO (*m/z* 44 and 28, respectively) varied with

the voltage oscillations. Overall, we observed that oscillations in the anodic overpotential are in phase with that of the CO and CO<sub>2</sub> signals. This fact is consistent with an autonomous adsorption–oxidation cyclic process. For both anodes, it has been observed that, in general, an increase in current density implies an increase in oscillatory frequency. By using CO stripping, we also discuss how the onset of CO oxidation is related to the maximum overpotential reached during a cycle, whereas the minimum overpotential can be associated with the catalytic activity of the electrode for H<sub>2</sub> oxidation.

## 1. Introduction


Polymer electrolyte membrane fuel cells (PEMFCs) are devices that convert the chemical energy of hydrogen or other fuels and oxygen directly into electrical energy. In the case of hydrogen, an important limitation is the source of hydrogen used because when hydrogen is generated by hydrocarbon reformation, CO is produced concomitantly and remains as a contaminant.<sup>[1]</sup> Even very low concentrations of carbon monoxide in the anode fuel can result in a severe decrease in energy conversion efficiency.<sup>[2–5]</sup> Strategies inspired by the use of a second metal in Pt-based anode catalysts have been explored as potential routes to increase the CO tolerance relative to pure Pt.<sup>[2,5–12]</sup> Within the possibilities of bimetallic electrocatalysts, Pt-Ru shows great activity for H<sub>2</sub> oxidation in the presence of CO and it is the most successful alloy characterized to date.<sup>[11]</sup> An interesting aspect of these devices is that the reactions that occur on the surface of these catalysts and the adsorption/desorption processes are interrelated through the anode potential, and this delicate interplay can result in oscillatory behavior.<sup>[13–15]</sup> In addition, oscillatory dynamics in a PEMFC are not restricted to systems with a Pt-Ru/C anode,<sup>[16–28]</sup> and the occur-


rence on Pd-Pt/C<sup>[29]</sup> and on Pt<sup>[30,31]</sup> anodes has also been reported.

From a technical point of view, the occurrence of oscillatory kinetics can be thought of as an autonomous self-cleaning process<sup>[32]</sup> that can prevent the anode becoming completely poisoned by adsorbed carbon monoxide, as is the case under conventional, non-oscillatory conditions. In fact, it has been reported that operating a fuel cell under an oscillatory regime can result in higher average power densities than those obtained at a steady state.<sup>[17,23–26,29–31]</sup>

An interesting way to study the reaction mechanisms involved in such systems is by combining the results of potential variation over time with another technique, such as on-line mass spectrometry (OLMS). The model proposed by Zhang et al.<sup>[19]</sup> in 2004 demonstrated the relationship between the anodic overpotential and the CO<sub>ad</sub> coverage, and also showed that OH<sub>ad</sub> and H<sub>ad</sub> coverage are essential variables for the occurrence of oscillations. However, the temporal dependence of the molar fraction of CO ( $\chi_{\text{CO}}$ ) at the anode outlet was considered not to be essential for the occurrence of oscillations, that is, even with  $\chi_{\text{CO}}$  kept constant, the model still exhibited oscillatory behavior. To verify if the anodic CO concentration oscillates simultaneously with the overpotential, the authors used an on-line infrared gas analyzer; however, they did not observe oscillations in the CO concentration at the anode outlet stream. They raised the possibility that either  $\chi_{\text{CO}}$  did not in fact oscillate or the resolution of the gas analyzer was too low for the oscillatory frequencies evaluated. Lopes et al.<sup>[21]</sup> modified the model proposed by Zhang et al.<sup>[19]</sup> by including the CO<sub>2</sub> mass balance within the anode channel. They employed a mass spectrometer coupled to the gas outlet of the anode and monitored the *m/z* value of 44 amu (atomic mass unit), which is related to CO<sub>2</sub>. With this experimental setup, they

[a] J. A. Nogueira, Prof. Dr. H. Varela  
Institute of Chemistry of São Carlos  
University of São Paulo  
POBox 780, 13560-970, São Carlos, SP (Brazil)  
E-mail: hamiltonvarela@usp.br

 The ORCID identification number(s) for the author(s) of this article can be found under <https://doi.org/10.1002/open.201700098>.

 © 2017 The Authors. Published by Wiley-VCH Verlag GmbH & Co. KGaA. This is an open access article under the terms of the Creative Commons Attribution-NonCommercial-NoDerivs License, which permits use and distribution in any medium, provided the original work is properly cited, the use is non-commercial and no modifications or adaptations are made.

demonstrated the occurrence of oscillations in CO<sub>2</sub> production that are in phase with the cell potential oscillations when Pt/Ru/C was the anode catalyst. However, *m/z* 28 was not evaluated, although it has contributions from both CO and CO<sub>2</sub> because it is a fragment produced from the CO<sub>2</sub> ionization process. Bearing in mind that part of the ionic current related to *m/z* 28 comes from the fragmentation process of *m/z* 44<sup>[33]</sup> and assuming no influence due to atmospheric N<sub>2</sub>, we chose to follow both *m/z* 28 and 44 and thus observe how the profiles associated with CO and CO<sub>2</sub> varied during the oscillatory operation of the PEMFC. Overall, a careful analysis of the oscillatory dynamics in PEMFC is of interest not only from fundamental perspective, but is also essential to enhance operation and process design.

Herein, we explore the dynamics of a PEMFC equipped with Pd-Pt/C and Pd/C anodes and fed with H<sub>2</sub>/CO. Experiments were carried out under galvanostatic control and, concomitantly with the potential oscillations, we also followed the temporal evolution of CO consumption and CO<sub>2</sub> production by using on-line mass spectrometry. By simultaneously measuring the potential and the signals attributed to CO and CO<sub>2</sub>, it is possible to provide a more comprehensive experimental view of the processes involved in the oscillatory kinetics of a PEMFC. In particular, it became evident that the  $\chi_{\text{CO}}$  value at the anode outlet in fact oscillates with the overpotential. Additionally, by using CO-stripping voltammetry, it was possible to correlate how the catalytic activity for hydrogen oxidation and CO oxidation affected the oscillation profile.

## 2. Results and Discussion

The EDX compositions of the Pd-Pt/C and Pd/C electrocatalysts are shown in Table 1. The average compositions were almost in agreement with the nominal compositions (i.e. the relative amounts of metallic precursors used in synthesis).

The XRD patterns of Pt/C (E-TEK), Pt/C, Pd-Pt/C, and Pd/C are shown in Figure 1, and the lattice parameters and the average crystallite size, as estimated from the XRD data by using the Scherrer equation, are included in Table 1. The results for Pt/C (E-TEK) are reported for comparison. The broad peak at approximately 25° corresponds to the (002) plane of the hexagonal structure of the carbon support, in this case Vulcan XC-72 carbon (Cabot). The remaining peaks indicated in Figure 1 are related to diffraction from the (111), (200), (220), and (311)

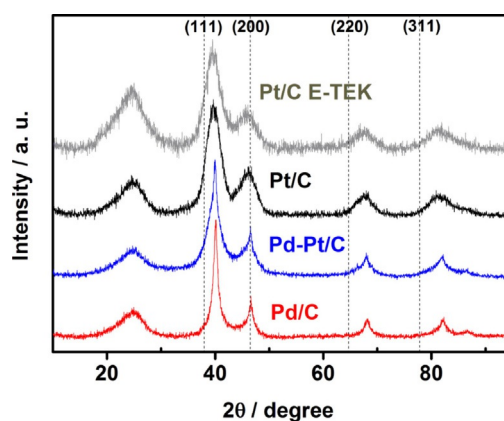


**Figure 1.** X-ray diffractograms for Pt/C E-TEK, Pt/C, Pd-Pt/C, and Pd/C catalysts;  $\lambda = 1.5406 \text{ \AA}$  (Cu<sub>K $\alpha$</sub> ).

planes, respectively, which represent the face-centered cubic (fcc) phase, a typical structure of the palladium or platinum metals. It was observed that the peaks of the Pd-containing materials are narrower and more intense, which is evidence for larger crystallite sizes than Pt/C and can also be observed from the crystalline size shown in Table 1. It is worth noting that Pd and Pt have similar atomic sizes and identical crystalline structure, and this explains their similar diffraction peaks. The lattice parameter value of Pd-Pt/C (0.3901 nm) is slightly larger than that of pure Pd (0.3891 nm) and smaller than that for Pt/C, which suggests the formation of a Pd-Pt/C alloy. The average crystallite size of the Pd-Pt/C catalyst (6.5 nm) is more than twice that of Pt/C obtained by the same method (2.7 nm). In general, the crystallite size of carbon-supported metals increases in the order Pt < Pd-Pt < Pd,<sup>[10,34]</sup> and the different sizes and dispersions observed for metal nanoparticles on a carbon support are, above all, due to different nucleation mechanisms for Pt and Pd.<sup>[34]</sup>

The performance of the PEMFC is presented in Figure 2 in terms of the steady-state polarization curves obtained by using Pd/C, Pd-Pt/C, and Pt/C anodes, and fed with H<sub>2</sub> or H<sub>2</sub>/CO at 30 °C and an anode flow rate of 150 sccm. The activity towards the electrooxidation of hydrogen in the absence of carbon monoxide (Figure 2) decreased in the sequence Pt/C > Pd-Pt/C > Pd/C. The poor activity of Pd/C is in agreement with others studies, which have shown that, in general, Pd/C performs H<sub>2</sub> oxidation poorly compared with Pt/C.<sup>[10,11,34]</sup> It is known that the presence of platinum, even in tiny amounts, considerably increases the overall catalyst activity,<sup>[34]</sup> but only a small enhancement has been observed here for the Pd-Pt/C anode. This poor improvement is likely due to the considerably low temperature used (30 °C).

When H<sub>2</sub> contaminated with CO (100 ppm) was used instead of pure H<sub>2</sub>, all catalysts showed an appreciable performance decrease, as can be seen in Figure 2b. The system with the Pd/C anode showed the worst performance of all the electrocatalysts evaluated because the current for this catalyst was almost suppressed by the addition of CO. For the Pt/C catalyst, this decrease is well reported in the literature.<sup>[2–12]</sup> This loss in efficiency is due to the strong adsorption of CO on the surface

**Table 1.** Physical parameters for anodes of 20 wt% Pt/C E-TEK, Pt/C, Pd-Pt/C, and Pd/C, prepared by using the formic acid reduction method, obtained from EDX and XRD analysis.

| Catalyst  | EDX, Pd [at%] | EDX, Pt [at%] | XRD crystallite size [nm] <sup>[a]</sup> | XRD lattice parameter [nm] <sup>[a]</sup> |
|-----------|---------------|---------------|--|---|
| Pt/C ETEK | —             | 100           | 2.3                                      | 0.3926                                    |
| Pt/C      | —             | 100           | 2.7                                      | 0.3920                                    |
| Pd-Pt/C   | 48.55         | 51.45         | 6.5                                      | 0.3901                                    |
| Pd/C      | 100           | —             | 7.0                                      | 0.3891                                    |

[a] Estimated by using the Scherrer equation.

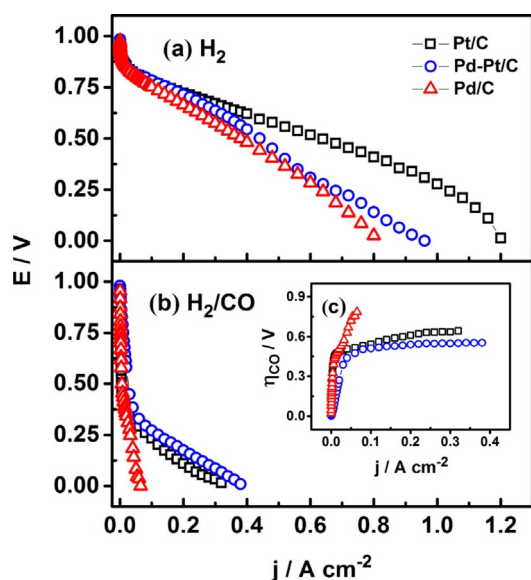


**Figure 2.** Steady-state polarization curves for cells equipped with Pd-Pt/C (○), Pd/C (△), and Pt/C (□) as anode catalysts when fed with a) H<sub>2</sub> or b) H<sub>2</sub>/100 ppm CO. c) The overpotential associated with the presence of carbon monoxide. Cathode: Pt/C, anode flow rate: 150 sccm, T = 30 °C.

of the catalyst, which inhibits the adsorption and oxidation of hydrogen. Conversely, the Pd-Pt/C anode gave current densities slightly higher than that of Pt. It has been reported that the inclusion of Pd in the Pt anode catalyst increases CO tolerance.<sup>[10,11,29,34]</sup> By using CO-stripping voltammetry, Papageorgopoulos et al.<sup>[11]</sup> and Garcia et al.<sup>[10]</sup> have shown that the main peak potential is shifted to more anodic values as the Pd proportion increases in Pd-Pt catalysts. This fact shows that the oxidative removal of CO on Pd-Pt/C surfaces is disadvantageous compared with Pt/C and that, in turn, the higher CO tolerance should be attributed to the electronic effect that Pd exerts on Pt.<sup>[10]</sup> By subtracting the curve obtained in the presence of the H<sub>2</sub>/CO mixture from that obtained with pure H<sub>2</sub>, it was possible to estimate the overpotential due to the presence of carbon monoxide, as shown in Figure 2c, from which it can be observed that the oxidation of CO only occurs above approximately 0.5 V for Pt/C and Pd-Pt/C, and the cell with Pd/C

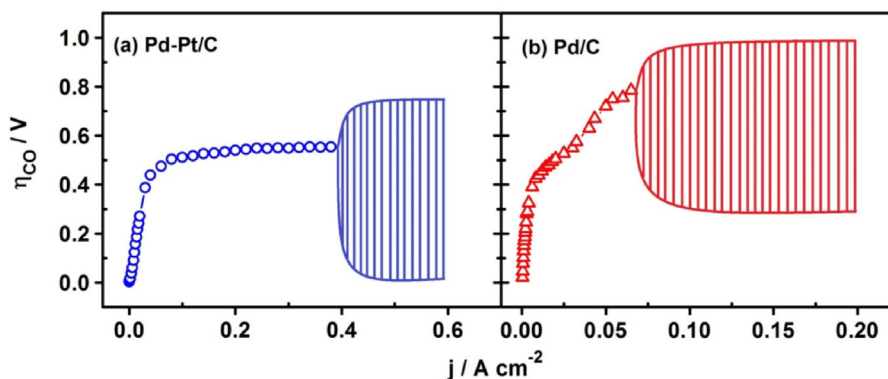
presented very low current densities even at high overpotentials.

Figure 3 presents the overpotentials for the Pd/C and Pd-Pt/C anodes determined from the data in Figure 2c, but in a wider current window. In addition to that in Figure 2c, it is shown in Figure 3 that the curve of the overpotential splits into two branches at a certain value of the applied current. At this point the system undergoes a bifurcation and the anodic potential starts oscillating spontaneously. The dashed area thus presents the oscillation amplitude at a given applied current.

The emergence of potential oscillations, as shown in Figure 3, occur because when a PEMFC is operated galvanostatically, the CO in the inlet gas adsorbs on the surface of the anodic catalyst and blocks free sites for H<sub>2</sub> electrooxidation. To maintain the applied current, the anodic overpotential increases gradually. At sufficiently high overpotentials, the electrooxidation rate of CO<sub>ad</sub> exceeds its adsorption rate and releases free sites, which allows the oxidation of H<sub>2</sub>. Given that the greatest contribution to faradaic current comes from the electrooxidation of H<sub>2</sub>,<sup>[19]</sup> the anodic overpotential decreases and the cycle starts anew.<sup>[18,19]</sup>

The oscillations in the anode overpotential for Pd-Pt/C as the anode catalyst with the respective CO<sub>2</sub> and CO signals are shown in Figure 4, whereas the results for Pd/C are presented in Figure 5. The OLMS data were normalized by assuming that the maximum is equal to 1 and the minimum to zero to obtain qualitative information on how the self-organized variation in potential interferes with the consumption/production of CO and CO<sub>2</sub>.

For all current densities evaluated within the oscillatory region, the PEMFC with a Pd-Pt/C anodic catalyst presented 2-period oscillations, with amplitudes between 0.70 and 0.80 V, whereas the frequency was dependent on the required current of the system (the higher the current, the higher the frequency). For the PEMFC with a Pd/C anode, oscillations began with 1-period and underwent a period-doubling bifurcation at an applied current greater than 0.22 A cm<sup>-2</sup> to present an amplitude of approximately 0.60 V, whereas the frequency, as for Pd-Pt/C, depended on the current. Figures 4 and 5 also show the normalized signals for CO and CO<sub>2</sub>, assigned to *m/z* 28 and 44,



**Figure 3.** Bifurcation diagrams in terms of overpotential for PEMFCs with a) Pd-Pt/C and b) Pd/C as the anode. Cathode: Pt/C, anode flow rate: 150 sccm, T = 30 °C.

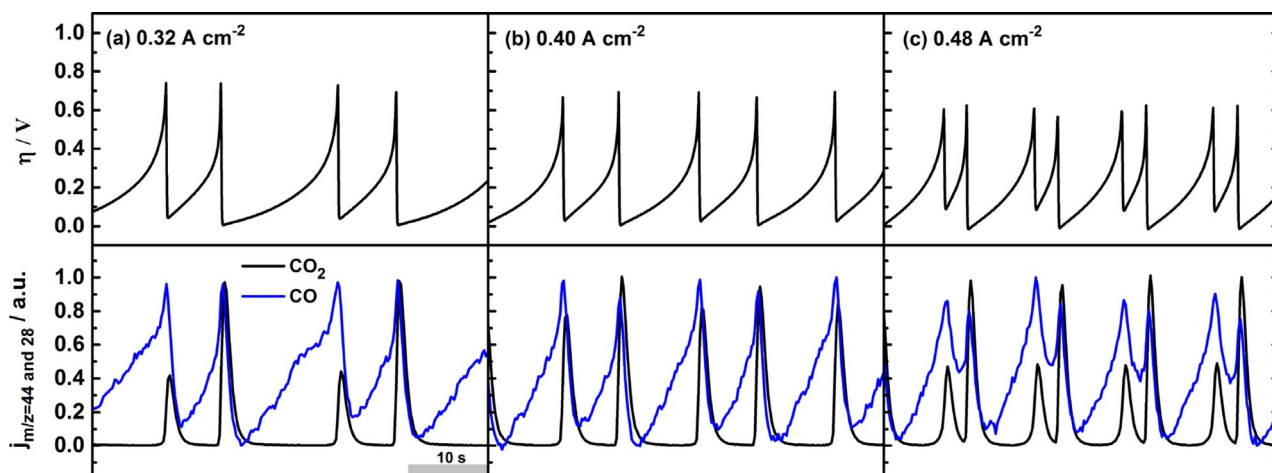


**Figure 4.** Oscillation with time of the anode overpotential (top) and of CO<sub>2</sub> and CO signal profiles (bottom) in the outlet flow measured by using OLMS for a PEMFC with a Pd-Pt/C anode at different current densities.

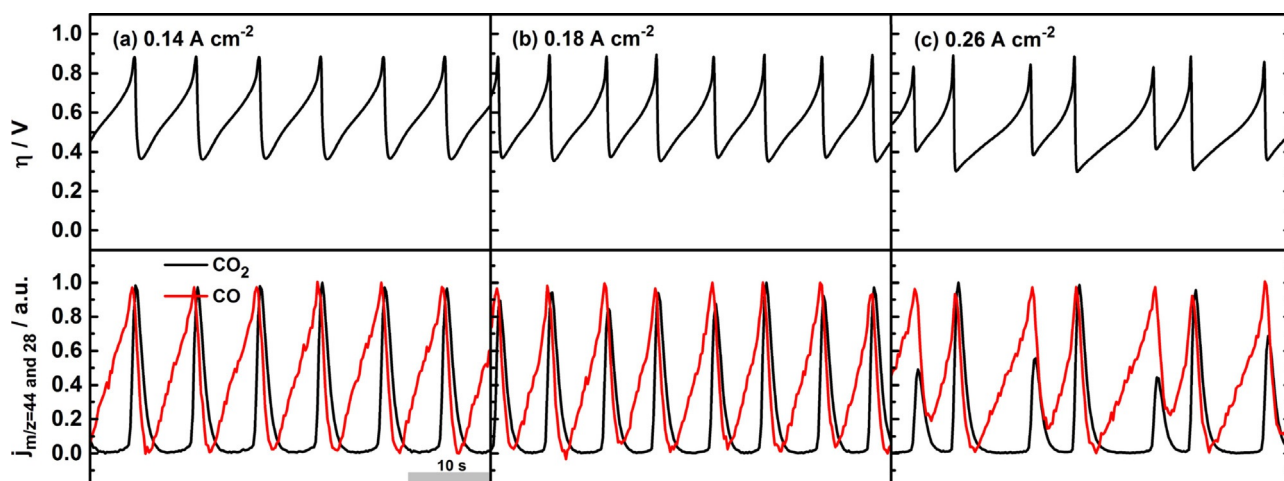


**Figure 5.** Oscillation with time of the anode overpotential (top) and of CO<sub>2</sub> and CO signal profiles (bottom) in the outlet flow measured by using OLMS for a PEMFC with a Pd/C anode at different current densities.

respectively. For both catalysts it can be observed that the maximum overpotential is in phase with the CO and CO<sub>2</sub> signals. First, looking at the  $m/z$  28 signal attributed to CO, it can be seen that when  $m/z$  44 is at a minimum and practically unchanged,  $m/z$  28 is in ascension. This fact is important because it gives us the assurance that the  $m/z$  28 signal is not just a reflection of the  $m/z$  44 signal. It can also be noted that the overpotential and CO<sub>2</sub> and CO signals assume different waveforms in the temporal evolution. For example, the CO waveform is saw-toothed whereas the CO<sub>2</sub> oscillations are spike-like. In a paper by Zhang and Datta,<sup>[18]</sup> the proposed model showed that  $\chi_{CO}$  oscillates in a narrow range of experimental conditions and, unlike the shape shown in Figures 4 and 5, the value of  $\chi_{CO}$  increased rapidly shortly after the overpotential peak, then increased slowly and very little, then decayed and the cycle began again. The fact that the CO signal obtained by using OLMS increased almost linearly during the electrode poisoning process may provide mechanistic information, such as

the adsorption rate of CO on different electrocatalysts. However, one should keep in mind the sensitivity and resolution of the technique for CO detection to avoid misinterpretations. However, the advance obtained from the experimental point of view should be highlighted, as is evident from Figures 4 and 5 that the  $\chi_{CO}$  value in the anodic outlet in fact oscillates with the potential, which complements the works of Zhang et al.<sup>[19]</sup> and Lopes et al.<sup>[21]</sup> These results can be interpreted as follows: when the overpotential is at its minimum value, the electrocatalyst has free sites that allows H<sub>2</sub> electrooxidation; however, CO adsorbs strongly on both Pd-Pt/C and Pd/C and causes the anodic overpotential to increase to maintain constant current. When the overpotential is high enough, the formation of oxygenated species on the surface of the catalysts begins, which allows the oxidation of CO<sub>ad</sub> to CO<sub>2</sub> by the Langmuir–Hinshelwood mechanism.<sup>[2–9]</sup> This is corroborated by the OLMS data, in which the maximum overpotential coincides with the peak of CO<sub>2</sub> production. The oxidation of CO<sub>ad</sub> releases free sites

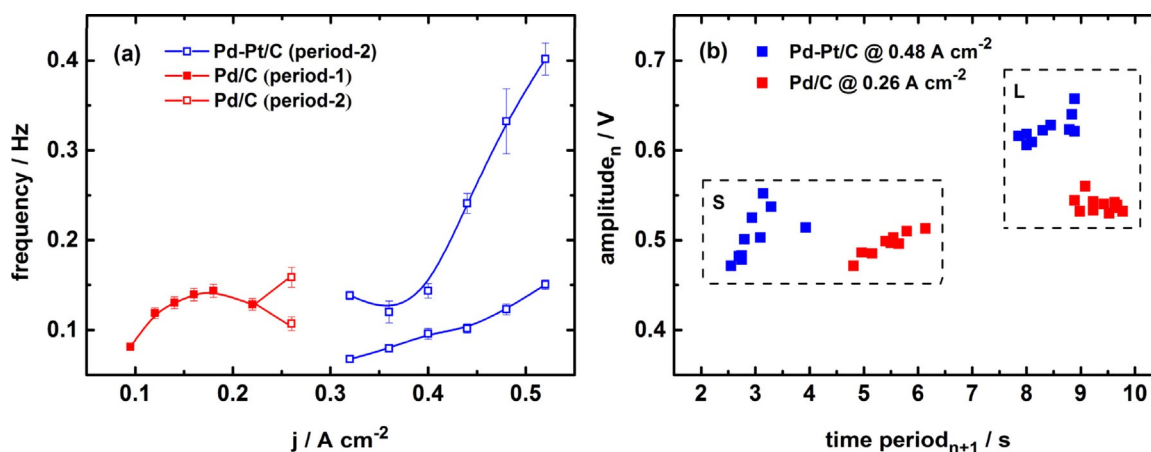


**Figure 6.** a) Oscillation frequency as a function of cell current for PEMFCs with Pd-Pt/C (blue) and Pd/C anodes (red). b) Oscillation amplitude (S = small and L = large) versus the time period needed for the next overpotential spike.

and in turn causes the overpotential to decay rapidly, as does the CO signal. The decrease in the CO signal is due to the fact that free sites are available for its re-adsorption, which leads to a decrease in its molar fraction within the anode channel.

Figure 6a shows how the oscillatory frequency changes as the current increases, whereas Figure 6b presents an analysis introduced by Mota et al.,<sup>[16]</sup> in which the oscillation amplitude of a given cycle is a function of the time spent before the potential spike in this cycle,  $t_{n+1}$ . It is worth noting that the tendency observed for Pd-Pt/C and also for Pd/C up to  $0.18 \text{ A cm}^{-2}$  (see Figure 6a), at which an increase in current leads to an increase in oscillatory frequency is in contrast to the model proposed by Lopes et al.<sup>[21]</sup> to explain the oscillatory dynamics in PEMFC with a Pt-Ru/C anode, for which an increase in current density for the same  $\text{H}_2$  flow led to slower oscillations. They explained this trend based on the fact that the greater the overpotential, the greater the  $\text{CO}_2$  production. As the current is increased, the turnover rate of the  $\text{H}_2$  electrooxidation increases and this may lead to an increase in the overpotential, which in turn leads to a greater conversion of  $\text{CO}_{\text{ad}}$  to  $\text{CO}_2$ . This higher conversion decreases the CO partial pressure and consequently the oscillation frequency because there is longer period before critical CO coverage is reached. In another study with Pd-Pt/C,<sup>[29]</sup> the authors explained the increase in frequency with increased current (as in Figure 6a) by assuming that for low flow and high current densities, high consumption of  $\text{H}_2$  leads to an increase in the CO concentration within the anode chamber, which in principle is also true for the Pt-Ru/C anode. Kadyk et al.<sup>[30]</sup> evaluated the oscillatory behavior in PEMFC with a Pt anode and observed that the oscillations had high frequency near the bifurcation but decreased considerably until they reached an almost constant value at high current densities. Another observation is that the higher the CO concentration, the higher the frequency, which agrees with the explanation given by Lopes et al.<sup>[29]</sup> These previous studies have identified two kinds of trends, that is, for Pt and Pt-Ru/C anodes an increase in current leads to a decrease in oscillatory frequency, whereas for Pd-Pt/C anodes an increase in frequency occurs. Considering the electrocatalysts evaluated

here, it is not simple to point out why an increase in current leads to an increase in frequency, but one possibility would be the lower catalytic activity of Pd-Pt/C and Pd/C for the CO oxidation reaction. This makes all processes that contribute to the faradaic current increase in speed to maintain a constant current. For example, following the hypothesis that the higher the current, the higher the rates of all steps involved, the adsorption rate also increases or the critical coverage of  $\text{CO}_{\text{ad}}$  required for the next cycle decreases, which consequently leads to a decrease in the period.

As already mentioned, it can be observed in Figure 6a that for a PEMFC with a Pd/C anode oscillations begin with 1-period, then above  $0.18 \text{ A cm}^{-2}$  there is a small decrease in frequency, and the system undergoes a second bifurcation above  $0.22 \text{ A cm}^{-2}$  to 2-period. In contrast, for the system with a Pd-Pt/C anode the dynamic begins as 2-period. Hanke-Rauschenback et al.<sup>[20]</sup> addressed oscillations and pattern formation in PEMFCs with a PtRu anode fed with  $\text{H}_2/\text{CO}$  by using a one-dimensional isothermal model and found that if the system is limited by CO transport within the anodic chamber rather than being limited by CO adsorption, the system shows period-doubling. It is interesting to note that the emergence of 2-period oscillations for Pd/C above  $0.22 \text{ A cm}^{-2}$  and for Pd-Pt/C at all currents evaluated occurred at a relatively high inlet flow rate of 150 sccm. For example, Mota et al.<sup>[16]</sup> observed period-doubling at 50 and 20 sccm with PtRu/C and Lopes et al.<sup>[29]</sup> observed period-doubling for Pd-Pt/C at 24 sccm. Therefore, we can raise the possibility that in the case of the Pd/C anode, the second bifurcation is due to the distance from equilibrium, which causes two processes to overlap to supply the applied current, and in the case of Pd-Pt/C this may be due to the inhomogeneity of the catalyst surface (i.e. distinct processes occurring over Pt and over Pd). However, given the experimental setup used herein, it was not possible to obtain spatially resolved information for the electrodes. In addition, when both catalysts exhibited 2-period oscillations (Figure 6b), we note a typical trend in which the smaller the oscillation amplitude, the shorter the time needed for the next overpotential spike. This fact can be understood as follows: smaller ampli-

tudes are less effective for CO<sub>ad</sub> oxidation and reduce the time required to obtain critical CO coverage for the next cycle.<sup>[16,20,29]</sup> In this specific case, we can use the expression derived by Kadyk et al. [Eq. (1)].<sup>[30]</sup>

$$t_{\text{CO,ad}} \approx \frac{\gamma C_t^* (\theta_{\text{CO}}^{\text{max}}(T) - \theta_{\text{CO}}^{\text{min}}(T))}{K_{\text{CO,ad}}(T) \bar{\theta}_0(T) \chi_{\text{CO}} p} \quad (1)$$

in which  $t_{\text{CO,ad}}$  is the time for CO adsorption (this term is approximately equal to the period of one cycle);  $\gamma C_t^*$  is the number of catalyst sites and  $\gamma$  is the roughness factor;  $K_{\text{CO,ad}}(T)$  is the rate constant of CO adsorption;  $\bar{\theta}_0(T)$  is the average number of free surface sites;  $\theta_{\text{CO}}^{\text{max}}(T)$  is the maximum CO coverage and  $\theta_{\text{CO}}^{\text{min}}(T)$  is the minimum;  $\chi_{\text{CO}}$  is the molar fraction of CO and  $p$  is the pressure of the inlet gas. The greater the amount of CO<sub>ad</sub> remaining after one cycle, that is, the larger the value of  $\theta_{\text{CO}}^{\text{min}}(T)$  (assuming  $0 < \theta_{\text{CO}}^{\text{min}} < 1$ ), the smaller the poisoning time or  $t_{\text{CO,ad}}$  and, consequently, the next potential peak.

It can be seen that the differences between the Pd-Pt/C and Pd/C systems studied herein, and their differences relative to the Pt-Ru/C system, which is widely discussed in the literature,<sup>[6,16–28]</sup> reflect different adsorption/oxidation kinetic constants of CO and of H<sub>2</sub>, in addition to the H<sub>2</sub>O dissociation on the catalyst surface for the formation of OH<sub>ad</sub>. As first proposed by Lopes et al.,<sup>[29]</sup> CO-stripping voltammetry can be used to estimate the mean amplitude of oscillation. For PEMFCs with a Pt-Ru/C anode, the amplitude of the oscillations is around 0.45 V, a value that is similar to the potential of the CO oxidation peak on this electrode. With an anode of Pt/C, the CO oxidation peak is close to 0.7 V versus ERH, and this value was used by Zhang and Datta<sup>[19]</sup> to explain the absence of oscillatory instabilities for a cell with a Pt/C anode. However, Kadyk et al.<sup>[30]</sup> later observed potential oscillations in a PEMFC with a Pt black catalyst.

Figure 7 shows the results of CO stripping in the Pd-Pt/C and Pd/C anodes. For Pd-Pt/C the oxidation starts at about 0.80 V, whereas in Pd/C the oxidation begins at around 0.87 V. Looking at the overpotential time series (Figure 4), it is noted that for Pd-Pt/C the maximum overpotential reached is about 0.75 V and the minimum value is 0.0 V. For Pd/C, the maximum is around 0.85 V and the minimum is 0.35 V. We can rationalize this as follows: the maximum of the potential oscillations is related to the CO oxidation, and the onset potential of CO oxidation is a good indicator of this value, as shown by the results of CO stripping. The minimum is related to the H<sub>2</sub> oxidation, and because Pd/C is not as good an electrocatalyst as Pt for H<sub>2</sub> oxidation (see Figure 2a), it requires a greater overpotential than catalysts that contain Pt. The period is related to the CO adsorption process.

Finally, 2D attractors were constructed to explore the CO and CO<sub>2</sub> profiles during oscillations by correlating both signals, as shown in Figure 8 for two 2-period sets. Features common to both systems can be observed: maximum CO<sub>2</sub> production occurs when the CO signal assumes its highest value, and when CO<sub>2</sub> production is practically zero the CO signal increases.

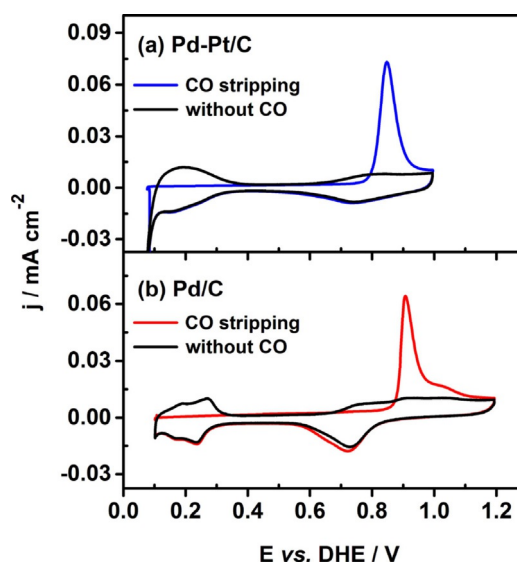


Figure 7. CO-stripping voltammetry of a) Pd-Pt/C and b) Pd/C catalysts. Adsorption period: 20 min at 0.1 V vs. DHE. After the adsorption period, excess CO was removed with Ar and then the potential was swept at 10 mV s<sup>-1</sup>.

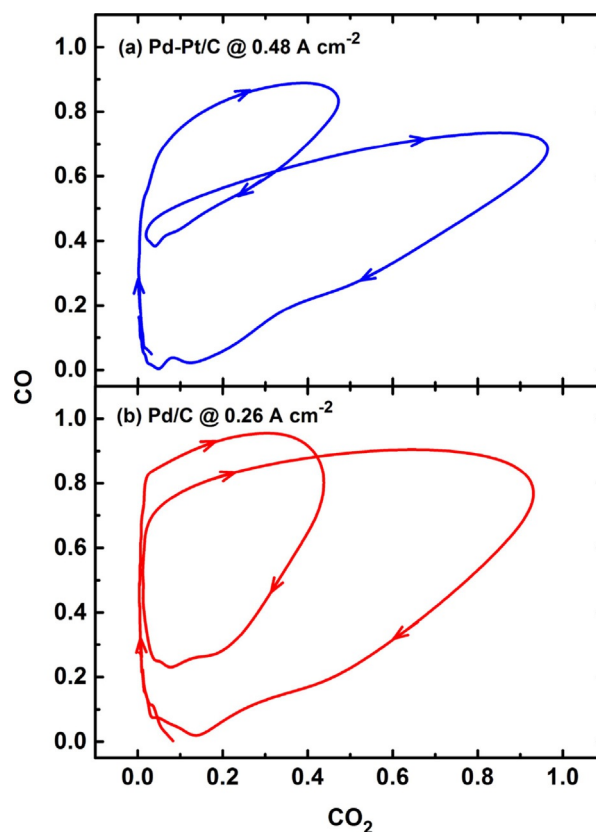


Figure 8. 2D attractors constructed by using the correlation between the signals assigned to CO and CO<sub>2</sub> for PEMFCs with a) Pd-Pt/C and b) Pd/C anodes.

es. This trend is in line with the fact that CO<sub>2</sub> production implies the release of active sites for the readsorption of CO, which causes the CO signal to decrease after the CO<sub>2</sub> maximum. Another point that deserves to be highlighted is that

the higher CO<sub>2</sub> production cycle is followed by a cycle of lower production in both cases when we evaluate the 2-period oscillations. Concomitantly, for the smaller-amplitude cycle, the CO signal does not go to zero, which agrees with the hypothesis first raised by Mota et al.<sup>[16]</sup> that the smaller the amplitude, the smaller the extent of CO<sub>ad</sub> oxidation. In other words, a smaller amount of CO present in the anodic chamber will adsorb because there are less free sites.

### 3. Conclusions

We report the occurrence of oscillatory kinetics during the operation of a PEMFC fed with H<sub>2</sub>/CO and equipped with Pd/C and Pd-Pt/C anode. With the help of the OLMS technique, it was possible to follow the mass fragments *m/z* 44 and 28 assigned to CO<sub>2</sub> and CO, respectively, and thus to evaluate in more detail the processes involved in the anodic potential oscillations. The main conclusions can be summarized as follows: 1) Despite the challenges in quantifying the CO outlet, it was possible to obtain qualitative data on how the voltage oscillations influence the production/consumption of CO<sub>2</sub>/CO. 2) Voltage oscillations were observed with both Pd-Pt/C and Pd/C anodes. On Pd-Pt/C, only 2-period oscillations were observed, and on Pd/C the oscillations began with 1-period and underwent a period-doubling bifurcation at high current densities. 3) In both systems, as the current increased, there was an increase in oscillatory frequency, in contrast to the behavior reported for Pt-Ru/C and Pt/C anodes. This feature may have its origin in the lower catalytic activity of Pd-Pt/C and Pd/C (at 30 °C) for CO electrooxidation, which possibly causes an increase in the speed of all reaction steps to maintain the applied current. 4) CO-stripping experiments allowed us to conclude that the onset potential for CO oxidation is a good indicator of the maximum overpotential reached during the oscillations. In turn, the minimum is related to the H<sub>2</sub> oxidation, whereas the period is related to the CO adsorption process.

### Experimental Section

Catalysts with 20 wt% Pd-Pt/C and Pd/C (i.e. 20 wt% metal on carbon) were prepared by reduction of the metal precursors with formic acid. They were prepared as follows: An appropriate amount of carbon powder (Vulcan XC-72, Cabot) was suspended in aqueous formic acid solution (0.5 mol L<sup>-1</sup>) and the suspension was heated to 80 °C. The metal precursors (H<sub>2</sub>PtCl<sub>6</sub>·6H<sub>2</sub>O and/or (NH<sub>4</sub>)<sub>2</sub>PdCl<sub>6</sub>; Alfa Aesar) were dissolved in high-purity water (Millipore Milli-Q, 18 MΩ cm), and this solution was added drop-wise with stirring to the carbon suspension. The suspension was left to cool at RT and the solid was filtered and dried in an oven at 80 °C for 1 h.<sup>[10]</sup>

The final compositions of the catalysts were determined by using the energy-dispersive X-ray (EDX) technique coupled to a scanning electron microscope (LEO Mod. 440) equipped with a SiLi detector and a 20 keV electron beam. Additionally, X-ray diffractograms (XRD) of the electrocatalysts were obtained by using a Rigaku model Ultima IV Diffractometer with an incident wavelength of 1.5406 Å (Cu<sub>Kα</sub>).

All experiments were conducted in a single-cell PEM with home-made Pd-Pt/C or Pd/C (20 wt%) catalysts as the anode and Pt/C (20 wt%; E-TEK) as the cathode. The metal loading was 0.4 mg<sub>M</sub> cm<sup>-2</sup> at both anode and cathode. The electrode and membrane electrode assembly (MEA) preparation are described elsewhere.<sup>[35]</sup> The electrochemical experiments were conducted in a unit cell (geometric area 4.62 cm<sup>2</sup>) at a constant temperature of 30 °C. To control cell humidification, the cell was first activated and humidified at 85 °C for 2 h at 700 mV with H<sub>2</sub>. Subsequently, the temperature was lowered to 30 °C and the MEA was saturated with H<sub>2</sub>/100 ppm CO mixture for 2 h at 800 mV. The anode flow rate was 150 sccm for all experiments. Pure oxygen (99.5%) was used as the cathode feed. All gases were purchased from White Martins. The flow rate was controlled by using a MKS Type 1179 mass-flow controller and a MKS Type 247 control unit. The polarization experiments in the PEMFC were carried out galvanostatically (Electronic Load HP 6050A) and potential oscillations were registered at a fixed cell current by using a Minipa ET-2615 digital multimeter. The anode overpotential related to the presence of CO was calculated by subtracting the cell potential for the cell operated with pure hydrogen from the potential in the presence of CO ( $\eta_{\text{CO}} = E_{\text{H}_2} - E_{\text{H}_2/\text{CO}}$ ). Details regarding the measurements by using an on-line mass spectrometer are available elsewhere.<sup>[6,9]</sup> The mass/charge (*m/z*) ratios 44 and 28 amu (atomic mass unit), related to CO<sub>2</sub> and CO, respectively, were monitored. Although fragment 28 also has a contribution from the ionization process of CO<sub>2</sub>, its measurement provides important information regarding the dynamic behavior of the system.

CO stripping voltammetry was performed to obtain the CO oxidation potential for Pd-Pt/C and Pd/C. The anode was used as the working electrode fed with Ar, whereas the cathode, fed with H<sub>2</sub>, was used as a dynamic hydrogen electrode (DHE). The working electrode (Pd-Pt/C or Pd/C) adsorbed CO for 20 min at 0.1 V vs. DHE at RT. Thereafter, the cell was flushed with Ar for 40 min to remove excess CO and the anode potential was scanned at 10 mV s<sup>-1</sup>.

### Acknowledgements

J.A.N. and H.V. acknowledge the São Paulo Research Foundation (FAPESP) for a scholarship (grant no. 2015/09295-9) and financial support (grant nos. 2012/21204-0 and 2013/16930-7). H.V. (grant no. 306151/2010-3) acknowledges Conselho Nacional de Desenvolvimento Científico e Tecnológico (CNPq) for financial support. J.A.N. acknowledges Dr. Pietro Papa Lopes for fruitful discussions.

### Conflict of Interest

The authors declare no conflict of interest.

**Keywords:** electrochemistry · fuel cells · hydrogen · oscillations · polymer electrolyte membrane

- [1] M. Oertel, J. Schmitz, W. Weirich, D. Jendrysek-Neumann, R. Schulten, *Chem. Eng. Technol.* **1987**, *10*, 248–255.
- [2] S. M. M. Ehteshami, S. H. Chan, *Electrochim. Acta* **2013**, *93*, 334–345.
- [3] G. A. Camara, E. A. Ticianelli, S. Mukerjee, S. J. Lee, J. MCBreen, *J. Electrochem. Soc.* **2002**, *149*, A748–A753.
- [4] H. Igarashi, T. Fujino, M. Watanabe, *J. Electroanal. Chem.* **1995**, *391*, 119–123.

- [5] S. J. Lee, S. Mukerjee, E. A. Ticianelli, J. MCBreen, *Electrochim. Acta* **1999**, *44*, 3283–3293.
- [6] P. P. Lopes, E. A. Ticianelli, *J. Electroanal. Chem.* **2010**, *644*, 110–116.
- [7] H. A. Gasteiger, N. M. Markovic, P. N. Ross, *J. Phys. Chem.* **1995**, *99*, 8290–8301.
- [8] T. R. Ralph, M. P. Hogarth, *Platinum Met. Rev.* **2002**, *46*, 117–135.
- [9] T. C. M. Nepel, P. P. Lopes, V. A. Paganin, E. A. Ticianelli, *Electrochim. Acta* **2013**, *88*, 217–224.
- [10] A. C. Garcia, V. A. Paganin, E. A. Ticianelli, *Electrochim. Acta* **2008**, *53*, 4309–4315.
- [11] D. C. Papageorgopoulos, M. Keijzer, J. B. J. Veldhuis, F. A. De Bruijn, *J. Electrochem. Soc.* **2002**, *149*, A1400–A1404.
- [12] Y. V. Tolmachev, O. A. Petriil, *J. Solid State Electrochem.* **2017**, *21*, 613–639.
- [13] M. Eiswirth, J. Bürger, P. Strasser, G. Ertl, *J. Phys. Chem.* **1996**, *100*, 19118–19123.
- [14] H. Varela, K. Krischer, *Catal. Today* **2001**, *70*, 411–425.
- [15] K. Krischer, H. Varela in *Handbook of Fuel Cells: Fundamentals, Technology and Applications*, Vol. 2 (Eds.: W. Vielstich, H. Gasteiger, A. Lamm), John Wiley and Sons, Chichester, **2003**, pp. 679–701.
- [16] A. Mota, P. P. Lopes, E. A. Ticianelli, E. R. Gonzalez, H. Varela, *J. Electrochem. Soc.* **2010**, *157*, B1301–B1304.
- [17] A. Mota, M. Eiswirth, E. R. Gonzalez, *J. Phys. Chem. C* **2013**, *117*, 12495–12501.
- [18] J. Zhang, R. Datta, *J. Electrochem. Soc.* **2002**, *149*, A1423–A1431.
- [19] J. Zhang, J. D. Fehribach, R. Datta, *J. Electrochem. Soc.* **2004**, *151*, A689–A697.
- [20] R. Hanke-Rauschenbach, S. Kirsch, R. Kelling, C. Weinzierl, K. Sundmacher, *J. Electrochem. Soc.* **2010**, *157*, B1521–B1528.
- [21] P. P. Lopes, B. C. Batista, G. A. Saglietti, H. Varela, E. A. Ticianelli, *J. Solid State Electrochem.* **2013**, *17*, 1851–1859.
- [22] R. Hanke-Rauschenbach, M. Mangold, K. Sundmacher, *Rev. Chem. Eng.* **2011**, *27*, 23–52.
- [23] J. Zhang, R. Datta, *J. Electrochem. Soc.* **2005**, *152*, A1180–A1187.
- [24] J. Zhang, R. Datta, *Electrochem. Solid-State Lett.* **2004**, *7*, A37–A40.
- [25] H. Lu, L. Rihko-Struckmann, R. Hanke-Rauschenbach, K. Sundmacher, *Top. Catal.* **2008**, *51*, 89–97.
- [26] H. Lu, L. Rihko-Struckmann, K. Sundmacher, *Phys. Chem. Chem. Phys.* **2011**, *13*, 18179–18185.
- [27] S. Kirsch, R. Hanke-Rauschenbach, B. Stein, R. Kraume, K. Sundmacher, *J. Electrochem. Soc.* **2013**, *160*, F436–F446.
- [28] S. Kirsch, R. Hanke-Rauschenbach, K. Sundmacher, *J. Electrochem. Soc.* **2011**, *158*, B44–B53.
- [29] P. P. Lopes, E. A. Ticianelli, H. Varela, *J. Power Sources* **2011**, *196*, 84–89.
- [30] T. Kadyk, S. Kirsch, R. Hanke-Rauschenbach, K. Sundmacher, *Electrochim. Acta* **2011**, *56*, 10593–10602.
- [31] M. O. Ozdemir, U. Pasaogullari, *Int. J. Hydrogen Energy* **2016**, *41*, 10854–10869.
- [32] M. V. F. Delmonde, L. F. Sallum, N. Perini, E. R. Gonzalez, R. Schlöl, H. Varela, *J. Phys. Chem. C* **2016**, *120*, 22365–22374.
- [33] PFEIFFER VACUUM GMBH, Mass spectrometer catalogue, Asslar, Germany, **2005**, p. 115, <http://www.istcgroup.com/pdf/Mass%20Spectrometer%20Catalog%202005%20-%202007.pdf>.
- [34] R. Aantolini, S. C. Zignani, S. F. Santos, E. R. Gonzalez, *Electrochim. Acta* **2011**, *56*, 2299–2305.
- [35] V. A. Paganin, E. A. Ticianelli, E. R. Gonzalez, *J. Appl. Electrochem.* **1996**, *26*, 297–305.

---

Received: May 18, 2017

Version of record online August 7, 2017